Analysis of the absorption and emission spectra of U4+ in α-ThBr 4

E. Simoni, S. Hubert, M. Genet

J. Phys. France **49** (1988) 1425-1434 AOÛT **1988,** PAGE 1425

Classification
Physics Abstracts
71.70C — 78.60

Analysis of the absorption and emission spectra of U^{4+} in α-$ThBr_4$

E. Simoni, S. Hubert and M. Genet

Institut de Physique Nucléaire, Laboratoire de Radiochimie, 91406 Orsay, France

(*Reçu le 3 décembre 1987, accepté le 13 avril 1988*)

Résumé. — La forme basse température α-$ThBr_4$ a une structure de type scheelite $I_{4_1/a}$ dans laquelle l'uranium tétravalent se substitue au thorium (symétrie de site S_4). En faisant l'hypothèse que l'état fondamental est Γ_4 comme dans la forme β-$ThBr_4$, les spectres d'absorption polarisés à 4,2 K montrent que D_{2d} est une bonne approximation. Cette matrice a la particularité d'exalter de très nombreuses fluorescences de U^{4+}, ce qui permet d'indexer quatre niveaux Stark de l'état fondamental $^3H_4$: Γ_5 à 110 cm^{-1}, Γ_1 à 473 cm^{-1}, Γ_1 à 623 cm^{-1} et Γ_5 à 830 cm^{-1}. 30 niveaux ont été indexés et les paramètres de champ cristallins de $U^{4+}(5f^2)$ ont été calculés dans l'approximation D_{2d} : $B_0^2 = -382$, $B_0^4 = -3\,262$, $B_4^4 = -1\,734$, $B_0^6 = -851$ et $B_4^6 = -1\,828$ cm^{-1}. Il est intéressant de montrer qu'une légère distorsion dans la structure scheelite α-$ThBr_4$ comparée avec la structure zircone β-$ThBr_4$ induit un changement important sur les paramètres de champ cristallin.

Abstract. — The low temperature form α-$ThBr_4$ has a scheelite structure $I_{4_1/a}$ in which the tetravalent uranium occupies the thorium site which is S_4. Assuming that the ground state remains Γ_4 as in the β-$ThBr_4$ form, the polarized absorption spectrum at 4.2 K shows that D_{2d} is a good approximation. A peculiarity of this host is the exaltation of very numerous fluorescences of U^{4+} which permit to assign four Stark levels of the ground state $^3H_4$: Γ_5 at 110 cm^{-1}, Γ_1 at 473 cm^{-1}, Γ_1 at 623 cm^{-1} and Γ_5 at 830 cm^{-1}. 30 levels have been assigned and the crystal field parameters of U^{4+} ($5f^2$) have been calculated in the D_{2d} approximation : $B_0^2 = -382$, $B_0^4 = -3\,262$, $B_4^4 = -1\,734$, $B_0^6 = -851$ and $B_4^6 = -1\,828$ cm^{-1}. It is interesting to note that a small distortion in the scheelite structure of the α-$ThBr_4$ compared with the zircon structure β-$ThBr_4$ induces important changes in the crystal field parameters.

1. Introduction.

Thorium tetrahalides (X = Cl, Br) possess numerous properties which make them attractive candidates for chemical, physical and spectroscopic studies.

Thorium tetrabromide and thorium tetrachloride have two polymorphic forms [1] with a transformation temperature of 426 °C for the former and 405 °C for the latter [2-3]. The high temperature form β-$ThBr_4$ isomorphous to β-$ThCl_4$ is characterized by the tetragonal zircon structure (space group $I_{4_1/amd}$) [4] and undergoes a phase transition at 90 K [5] with an incommensurate modulated structure below this temperature [6]. The low temperature form α-$ThBr_4$ isomorphous to α-$ThCl_4$ has the scheelite structure (space group $I_{4_1/a}$) [1].

From previous investigations of the solid state chemical properties of structural type [7], thorium has a D_{2d} site symmetry in the β-form of zircon structure, and S_4 site symmetry in the α-form of scheelite structure type. Large single crystals of pure and doped β-$ThBr_4$ may be grown easily by the Bridgman method [8], while the α-form is relatively difficult to prepare as a single crystal since the final form obtained by this way is the β-form. Additional studies of pure β-$ThBr_4$ have included X ray [9], neutron diffraction [6], Raman investigations [5] and complete analysis of crystal field parameters on U^{4+}, Pa^{4+}, Pr^{3+} diluted in the incommensurate modulated phase [10, 11, 12] of β-$ThBr_4$.

On the other hand only structural studies have been reported on the α-form of thorium tetrahalides [1, 2, 3, 7]. Recently nuclear quadrupole resonance investigations of Br^- [13] have shown that α-$ThBr_4$ keeps the same structure from room temperature down to 10 K and Raman scattering [14] has confirmed this result.

Some spectroscopic properties of trivalent rare earth ions in crystals with a scheelite structure have been already reported and the main interest in

crystals like $LiYF_4$, $PbMoO_4$ and $CaWO_4$ [15, 16] lies in their properties for laser materials. However these host materials are not the best candidates to study the spectroscopic properties of tetravalent actinides in the scheelite structure. Only tetravalent neptunium has been studied in $PbMoO_4$, and for the first time fluorescence has been observed [17, 18]. Like scheelite structure materials, these pure crystals exhibit good fluorescence when excited by U.V. radiation in the blue for β-$ThBr_4$ (zircon structure) [19] and red for α-$ThBr_4$ (scheelite structure) [20].

Thus α-$ThBr_4$ was chosen as a host material for spectroscopic properties of tetravalent uranium because it has the same structure and similar chemical and optical behaviour as the better known scheelite-structure tungstates and molybdates. On the other hand it is interesting to compare the spectroscopic properties of U^{4+} between β-$ThBr_4$ which has an incommensurate structure below 90 K with multisite continuum going from D_{2d} to D_2 [10] and α-$ThBr_4$ which has only one S_4 site.

In the present study, optical absorption and emission, Zeeman effect studies have been performed. Some fluorescence of U^{4+} has already been reported in β-$ThBr_4$ [21], β-$ThCl_4$ [22] and Cs_2ZrBr_6 [23], however in α-$ThBr_4$, numerous and very strong fluorescence lines from U^{4+} in the visible, as well as in the near infrared and infrared have been observed for the first time. The data have allowed reasonable energy level assignments. Parameters describing spin orbit coupling and crystal field interactions were adjusted using a least squares minimization procedure in the D_{2d} point group approximation. The calculations were made using a full diagonalization of the Hamiltonian matrix in the ($LSJJ_z$) representation. Good agreement was obtained between the observed and the calculated energies in spite of the D_{2d} approximation, as has already been reported in several papers concerning the scheelite structure materials [15, 24, 25].

2. Experimental procedure.

The α phase of doped $ThBr_4$ was synthetized by two techniques. Polycrystalline materials could be easily obtained by heating U^{4+} doped β-$ThBr_4$ single crystals or powder at 400 °C during one week. In any cases the final form was polycrystalline. On the other hand, only one green colored single crystal of α-$ThBr_4$ doped with about 25 ppm of U^{4+} has been obtained by the Bridgman method with the same conditions as for the β-form [8]. This single crystal was large enough to obtain linear polarization of the absorption spectra in the directions perpendicular and parallel to the crystal axes.

All the samples used for spectroscopic studies were analysed using X ray powder diffraction. In all the cases the X ray patterns showed a pure α phase.

Samples were hygroscopic and less stable than the β phase and were handled in an argon atmosphere glove box and enclosed in a silica tube under helium pressure.

The absorption and emission spectra in the visible and infrared were measured with the crystal excited by the full light emission produced by a 100 W iodine lamp and using a high resolution JOBIN YVON HR 1000 spectrometer (with a reciprocal dispersion of about 8 A/mm) at different temperatures ranging from 4.2 K up to 300 K. For detection, a Hamamatsu R374 photomultiplier was used in the visible region and a PbS photodiode was used in the infrared region. In the latter case the optical source was chopped and the detector signal measured by a PAR Model 186 A lock in amplifier. The wavelength readouts of the spectrometer were calibrated using various lines of the first and second order of Hg emission lines.

Samples were introduced in a variable temperature optical Dewar (Oxford Instrument) operating between 4.2 and 295 K. A temperature controller was used to set the temperature.

Laser excited fluorescence measurements were performed using a pulsed Sopra tunable dye laser pumped with a Sopra nitrogen laser.

Using a superconducting magnet, Zeeman splittings were recorded in the visible at 4.2 K with the crystal in a magnetic field of 6 T.

3. Theory and symmetry considerations.

The Th^{4+} ions in α-$ThBr_4$ which are substituted for by U^{4+} have S_4 point symmetry as in the well known scheelite structure.

An analysis of the crystal field parameters for the rare earth ions in scheelite calculated in D_{2d} and S_4 symmetry [15, 16] shows that taking S_4 symmetry as D_{2d} is a reasonable approximation. For this new host matrix we will show by selection rules in both symmetries that D_{2d} is a good approximation. In the D_{2d} symmetry all the crystal field parameters are real, whereas in the S_4 symmetry, the loss of symmetry elements results in the introduction of imaginary terms in the Hamiltonian : imB_4^4 and imB_4^6.

Assuming D_{2d} for S_4 symmetry amounts to neglect of both the imaginary crystal field parameters. The energy levels will be fitted by simultaneous diagonalization of the free ion and crystal field Hamiltonian H_{FI}, H_{CF} as described below.

Where :

$$H_{FI} = \sum_{k=2,4,6} f_k F^k + \zeta_{5f} \sum_i \mathbf{s}_i \mathbf{l}_i + \alpha L(L+1) + \beta G(G_2) + \gamma G(R_7) + \sum_{k=2,4,6} p_k P^k + \sum_{k=0,2,4} m_k M^k \quad (1)$$

$$H_{CF} = \sum_{k=2,4,6} B_0^k C_0^k + \sum_{k=4,6} B_4^k (C_4^k + C_{-4}^k) . \quad (2)$$

The F^k and ζ_{5f} represent respectively the radial parts of the electrostatic and spin orbit interaction between 5f electrons, α, β, γ are the parameters associated with the two-body effective operators of configuration interaction. The M^k and P^k parameters represent the spin-spin and spin other orbit interactions.

The classification of the experimental energy levels was made by analysing the polarisation data. According to the transformation properties of the electric dipole operator, identical axial and σ polarized spectra require the use of electric dipole selection rules while identical axial and π polarized spectra require the use of magnetic dipole selection rules. Since axial spectra could not be recorded, we assumed that electric dipole transitions predominate as for U^{4+} in β-$ThBr_4$ [21], β-$ThCl_4$ [22] and $ThSiO_4$ [27].

In examining the spectra, we will consider selection rules for D_{2d} point symmetry (S_4 is a subgroup of D_{2d}) as it has been made in the scheelite structure for the rare earth. If U^{4+} ion is in a D_{2d} symmetry site, the crystal field states are either singlet (Γ_1, Γ_2, Γ_3, Γ_4) or doublets (Γ_5) and certain transitions would be forbidden as shown in table I. The corresponding identifications of the D_{2d} levels in S_4 notation are listed in table II.

Table I. — *Electric dipole selection rules in* S_4 *and* D_{2d}.

S_4	Γ_1	Γ_2	Γ_3	Γ_4		D_{2d}	Γ_1	Γ_2	Γ_3	Γ_4	Γ_5
Γ_1		π	σ	σ		Γ_1				π	σ
Γ_2	π		σ	σ		Γ_2			π		σ
Γ_3	σ	σ		π		Γ_3		π			σ
Γ_4	σ	σ	π			Γ_4	π				σ
Γ_5						Γ_5	σ	σ	σ	σ	π

Table II. — *Identification of the irreductible representations of the* D_{2d} *point group in* S_4 *notation.*

D_{2d}	Γ_1	Γ_2	Γ_3	Γ_4	Γ_5
S_4	Γ_1	Γ_1	Γ_2	Γ_2	$\Gamma_{3,4}$

When the local site symmetry is perturbed by a lower symmetry environment such as S_4, some of the forbiddenness should be lifted like $\Gamma_4 \rightarrow \Gamma_2$ transition in the D_{2d} representation ($\Gamma_2 \rightarrow \Gamma_1$ transition in S_4 representation).

4. Experimental results and analysis of the spectra.

Figures 1 show the absorption and emission spectra of tetravalent uranium in the visible, near infrared and infrared range at 4.2 K. The σ and π polarizations were obtained for the strongest lines since it was recorded with single crystal doped with only 25 ppm of U^{4+}. Unfortunately we did not observe polarization on the emission lines.

This is the first time that so many intense fluorescence lines are observed. We note that in the α-form, the lines are sharp (5-15 cm^{-1}), this was not the case in the incommensurate phase of β-$ThBr_4$ (40-80 cm^{-1} for σ lines) [10].

Nevertheless the absorption spectra of U^{4+} in α-$ThBr_4$ have roughly the same trend as in β-$ThBr_4$. Moreover some absorption lines present a phonon sideband structure on the high energy side below 200 cm^{-1} which indicates strong coupling between the electronic and vibronic states as in the d elements.

If we interpret the spectra under the assumption that D_{2d} is a good approximation for S_4 symmetry and that the $^3H_4$ ground state is Γ_4 as for U^{4+} in β-$ThBr_4$ [10], $ThCl_4$ [22], $ThSiO_4$ [27], we expect 13 π zero phonon lines and 19 σ zero phonon lines in the range 4 000-25 000 cm^{-1} deriving from $\Gamma_4 \rightarrow \Gamma_1$ and $\Gamma_4 \rightarrow \Gamma_5$ transitions. We observed 14 strong π lines and 9 strong σ lines in this region and some weak lines the polarisation of which could not be observed. The transition $\Gamma_4 \rightarrow \Gamma_2$ forbidden in D_{2d} should be allowed in the S_4 symmetry ($\Gamma_2 \rightarrow \Gamma_1$ transitions), which should raise the number of π predicted lines to 21.

In the region 22 000-19 000 cm^{-1} the π line at 21 601 cm^{-1} and the 2 σ lines at 20 034 cm^{-1} and 19 529 cm^{-1} were attributed to $^3P_2$ and $^1I_6$ components. By comparing the spectra of U^{4+} in α-$ThBr_4$ with those of U^{4+} in β-$ThBr_4$, $^3P_1$ is the only multiplet well isolated at about 17 000 cm^{-1}. In the σ spectrum, we observed the $^3P_1$ (Γ_5) level at 17 083 cm^{-1} while in the π spectrum the $^3P_1$ (Γ_2) is missing. This missing π transition as others ($\Gamma_4 \rightarrow \Gamma_2$) can be explained by considering the U^{4+} to be in S_4 symmetry site which is nearly D_{2d}. The observed emission line at 16 907 cm^{-1} has been attributed to the $^3P_1$ (Γ_2) $\rightarrow$ $^3H_4$ (Γ_5) transition since when the temperature is raised (80 K), an absorption line appears at the same energy. At the same time, some additional lines appear and particularly another one near the $^3P_1$ (Γ_5) state at 16 973 cm^{-1}. This hot line at 16 973 cm^{-1} was assigned to the $^3H_4$ (Γ_5) $\rightarrow$ $^3P_1$(Γ_5) transition. As a matter of fact, the observation of a large number of hot lines in the visible and infrared from 40 K indicates that the first excited ground state sublevel at 110 cm^{-1} could be Γ_5 like as U^{4+} in β-$ThBr_4$ [10], β-$ThCl_4$ [22], $ThSiO_4$ [27].

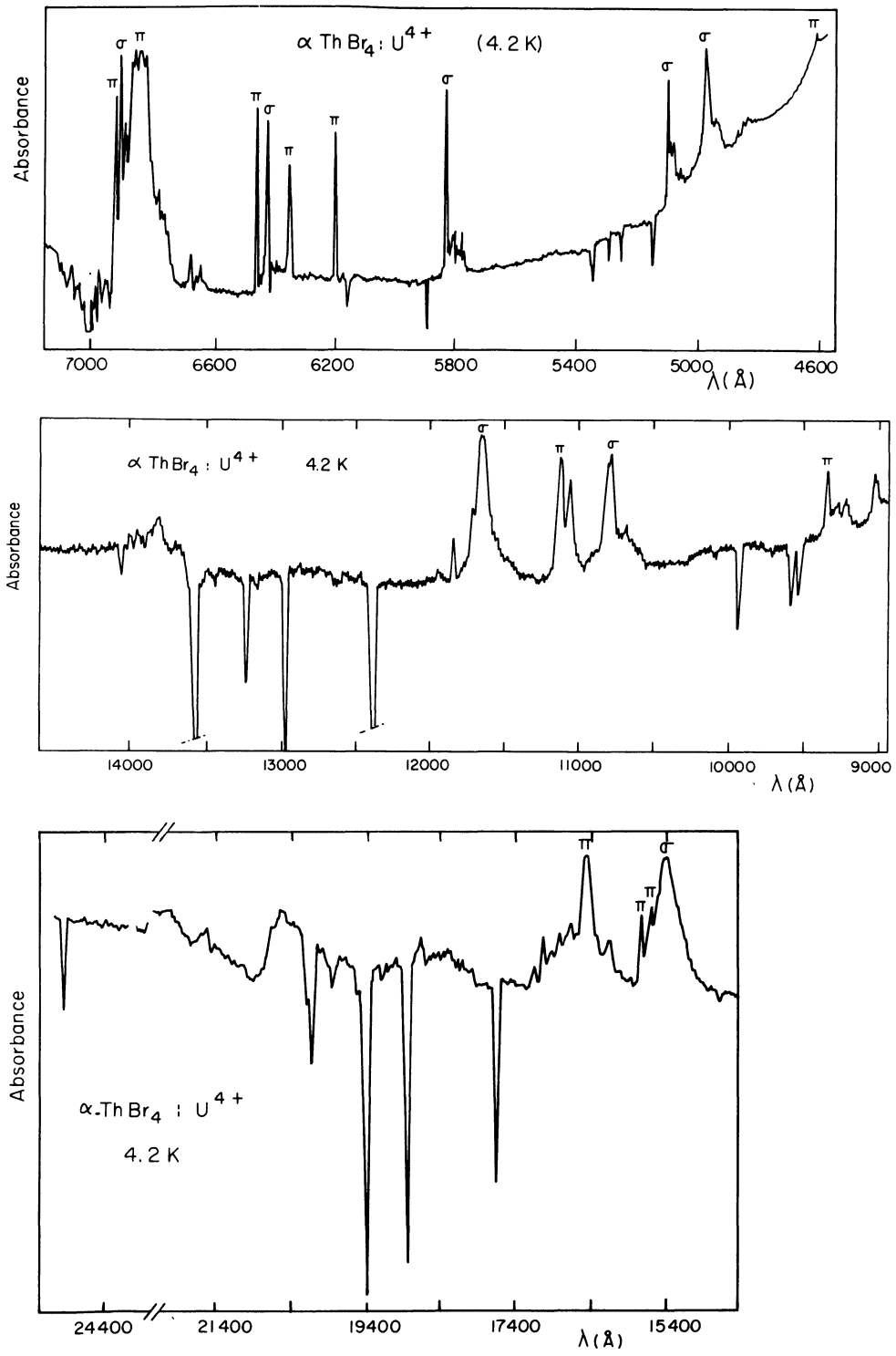

Fig. 1. — Absorption and emission spectra of α-$ThBr_4$: U^{4+} in the visible and infrared region at 4.2 K.

The Zeeman spectra proved to be particularly useful in identifying the Γ_5 lines. Using the magnetic field of 6 T at 4.2 K, Zeeman experiments indicated that the absorption line at 17 083 cm^{-1} is split which confirms the assignment of $^3P_1$ (Γ_5). Moreover by exciting the crystal with U.V. radiation from a nitrogen pumped laser, Zeeman splitting was also observed at 4.2 K in the emission spectrum. In particular the emission line at 16 907 cm^{-1} as well as two others at 19 329 and 14 219 cm^{-1} were clearly split into two components. These lines correspond, as we assumed above, to transitions between singlet states and the doubly degenerate state $^3H_4$ (Γ_5) at 110 cm^{-1}.

In the 15 000-16 000 cm^{-1} region, 3 strong π lines and one σ line were attributed to $^1G_4$ and $^1D_2$

multiplets. The strong π lines at 14 601, 14 573, 14 529 and 14 506 cm^{-1} were not assigned for the fitting.

For U^{4+} in β-$ThBr_4$, the $^3P_0$, $^1D_2$ and $^1G_4$ are close together. By comparison, the position of the $^3P_0$ (Γ_1) was established in the π spectrum at 14 389 cm^{-1}, while the strong σ line at 14 427 cm^{-1} was attributed to $^1D_2$ (Γ_5).

A peculiarity of the absorption and emission spectra of U^{4+} in this new host material is that most of the absorption lines like $^1I_6$ (Γ_5) at 19 529 cm^{-1}, the $^3P_1$ (Γ_5) at 17 083 cm^{-1}, the $^1D_2$ (Γ_1) at 14 389 cm^{-1}, the $^3H_6$ (Γ_5) at 10 647 cm^{-1}, the $^3F_3$ (Γ_5) at 8 558 cm^{-1} and the $^3H_5$ (Γ_1) at 6 076 cm^{-1} are followed on the low energy side by a set of 2, 3 or 4 strong fluorescent lines. When the crystal is excited with the Sopra nitrogen laser, the $^1I_6$ (Γ_5), the $^3P_1$ (Γ_5) and the $^3P_0$ (Γ_1) fluorescence as well, but with a weak intensity. In each group of emission, the energy difference between the fluorescent lines is the same as indicated in table III : 363, 513 and 720 cm^{-1}. When the temperature is raised from 4.2 K to 100 K, the highest energy emission lines from each group decrease faster in intensity than the other ones, and absorption lines rise up at the same energy like for $^3P_1$ (Γ_2). All these fluorescent lines come from different singlet excited levels near those labelled above, to reach 4 ground state Stark levels including the low lying one $^3H_4$ (Γ_5) at 110 cm^{-1}. Then we could deduce three other Stark levels to be at 473, 623 and 830 cm^{-1}. No Zeeman splitting was observed for the emission lines reaching these Stark levels. The fluorescences from each group reaching the $^3H_4$ state at 830 cm^{-1} could not be tested clearly since they are generally broad and weaker. However a slight broadening with magnetic field has been observed on one of them.

Selective excitation experiments with a tunable dye laser showed that each group of fluorescence lines comes from forbidden singlet excited levels very near the allowed lines observed in the absorption spectrum. From D_{2d} selection rules, and the energy position of the hot lines observable at 80 K, we could reach forbidden states and assign $^1I_6$ (Γ_4) at 19 439 cm^{-1}, $^3P_1$ (Γ_2) at 17 017 cm^{-1}, $^1D_2$ (Γ_4) at 14 355 cm^{-1}, $^1D_2$ (Γ_3) at 14 329 cm^{-1}, $^3H_6$ (Γ_4) at 10 504 cm^{-1}, $^3F_3$ (Γ_4) at 8 170 cm^{-1} and $^3H_5$ (Γ_4) at 5 765 cm^{-1}. Figure 2 represents the

Table III. — *Observed fluorescences of* U^{4+} *in* α-$ThBr_4$ *at* 4.2 K *towards* $^3H_4$ *ground state Stark levels.*

Initial multiplet	Wavelength (Å)	Wavenumber in vacuum (cm^{-1})	Energy difference (cm^{-1})
$^1I_6$ (1)	5 172	19 329 ([a,b])	0
	5 270	18 970	360
	5 313	18 816	513
	5 373	18 606	723
$^3P_1$ (2)	5 913	16 907 ([a,b])	0
	6 178	16 182	725
$^1D_2$ (3)	7 018	14 245 ([b])	0
	7 202	13 881	364
	7 393	13 522	723
$^1D_2$ (4)	7 031	14 219 ([a,b])	0
	7 406	13 499	720
$^3H_6$ (5)	9 618	10 394 ([b])	0
	9 966	10 031	363
	10 117	9 884	510
$^3F_3$ (6)	12 404	8 060 ([b])	0
	12 988	7 697	363
	13 246	7 547	513
	13 600	7 351	709
$^3H_5$ (7)	17 678	5 655	0
	18 888	5 293	363
	19 442	5 142	513
	20 260	4 934	721

([a]) Zeeman splitting observed.

([b]) Lines for which an absorption line rises when the temperature increases.

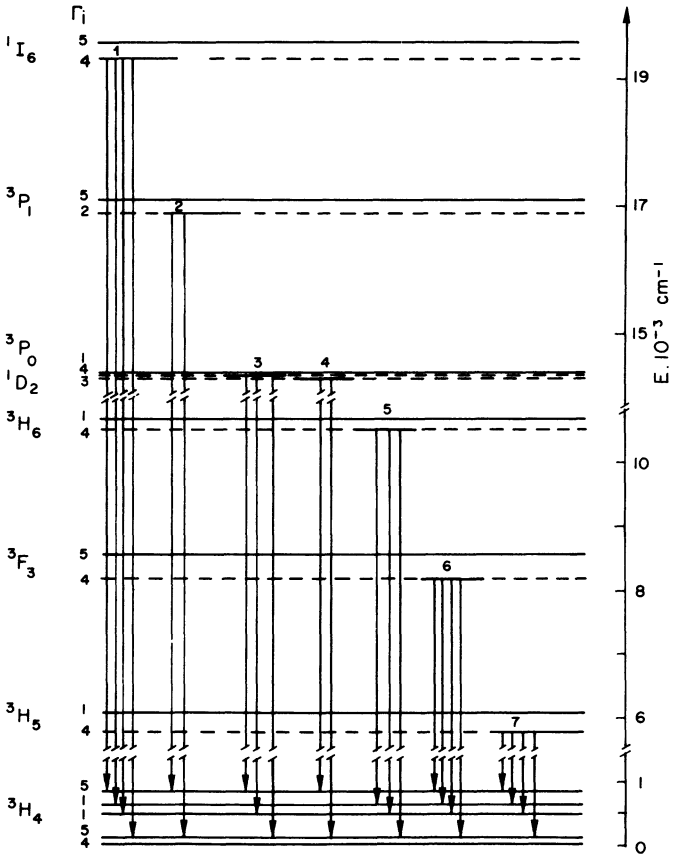

Fig. 2. — Partial energy level diagram for fluorescent transitions in α-$ThBr_4$: U^{4+}.

partial energy level diagram for fluorescent transitions reaching the $^3H_4$ levels in D_{2d} representation. The $^3H_4$ ground state Stark levels consist of $2\,\Gamma_1 + \Gamma_2 + \Gamma_3 + \Gamma_4 + 2\,\Gamma_5$ for D_{2d} point group symmetry. In the case where the emission lines are coming from Γ_4 states (group 1, 3, 5, 6, 7) the observation of 3 or 4 emissions indicates that these lines should correspond to $\Gamma_4 \rightarrow \Gamma_1$ and $\Gamma_4 \rightarrow \Gamma_5$ transitions. In the case where the emission lines are coming from Γ_2 or Γ_3 states, only two fluorescent lines are observed and correspond to $\Gamma_2 \rightarrow \Gamma_5$ or $\Gamma_3 \rightarrow \Gamma_5$ transitions. However in this case, the allowed transitions $\Gamma_2 \rightarrow \Gamma_3$ or $\Gamma_3 \rightarrow \Gamma_2$ are missing. From these considerations we attributed the Γ_5 symmetry to the $^3H_4$ Stark levels determined at 110 and 830 cm^{-1} and the Γ_1 symmetry to the $^3H_4$ Stark levels deduced at 473 and 623 cm^{-1}.

Table IV. — *Observed energy levels caracteristics for* α-$ThBr_4 : U^{4+}$.

λ (Å)	Energy (cm^{-1})	Polarization and intensity	D_{2d} assignment	S_4 assignment
4 531	22 064	W		
4 628	21 601	π M	Γ_1	Γ_1
4 990	20 034	σ	Γ_5	$\Gamma_{3,4}$
5 119	19 529	σ S	Γ_5	$\Gamma_{3,4}$
	19 439 (*)		Γ_4	Γ_2
5 852	17 083	σ	Γ_5	$\Gamma_{3,4}$
	17 017 (*)		Γ_2	Γ_1
6 222	16 067	π	Γ_1	Γ_1
6 371	15 692	π	Γ_1	Γ_1
6 446	15 509	σ	Γ_5	$\Gamma_{3,4}$
	15 456 (*)			
6 482	15 423	π S	Γ_1	Γ_1
6 847	14 601	π S	Γ_1	Γ_1
6 860	14 573	π S	Γ_1	Γ_1
6 881	14 529	π S	Γ_1	Γ_1
6 892	14 506	π S	Γ_1	Γ_1
6 913	14 460	π S	Γ_1	Γ_1
6 929	14 427	σ S	Γ_5	$\Gamma_{3,4}$
6 943	14 389	π S	Γ_1	Γ_1
	14 355 (*)		Γ_4	Γ_2
	14 329 (*)		Γ_3	Γ_2
9 072	11 020	M		
9 390	10 647	σ M	Γ_5	$\Gamma_{3,4}$
	10 504 (*)		Γ_4	Γ_2
10 820	9 240	σ S		
10 880	9 189	S	Γ_5	$\Gamma_{3,4}$
11 142	8 972	π S	Γ_1	Γ_1
11 682	8 558	σ S	Γ_5	$\Gamma_{3,4}$
11 736	8 518	W		
11 860	8 429	W		
	8 170 (*)		Γ_4	Γ_2
15 412	6 487	σ S	Γ_5	$\Gamma_{3,4}$
15 488	6 455	M		
15 596	6 410	π M	Γ_1	Γ_1
15 714	6 362	π M	Γ_1	Γ_1
16 452	6 076	π	Γ_1	Γ_1
	5 765 (*)		Γ_4	Γ_2
	830 (*)		Γ_5	$\Gamma_{3,4}$
	623 (*)		Γ_1	Γ_1
	473 (*)		Γ_1	Γ_1
	110 (*)		Γ_5	$\Gamma_{3,4}$

(*) Asterics indicate energy levels deduced from the fluorescence lines or from hot lines.

Results of fluorescence and absorption measurements are summarized in table IV. The table presents the line frequency in vacuo, the polarization, D_{2d} and S_4 symmetry assignment.

5. Discussion.

The levels were fitted by simultaneous diagonalization of the free ion H_{FI} and crystal field H_{CF} Hamiltonians describing the energy levels of U^{4+} in D_{2d} symmetry. Fitting the experimental levels with the starting parameters obtained for β-$ThBr_4 : U^{4+}$ [10] gives a very large *rms* deviation for α-$ThBr_4$. Using the β-$ThBr_4 : U^{4+}$ parameters, we diagonalized the matrices with various values of B_0^2. Only $B_0^2 \sim -400\ cm^{-1}$ gave the correct separation between the $^3P_1$ Γ_2 and Γ_5 levels. With this value for B_0^2, we tried to fit separately Γ_1 and Γ_5 levels. Both fits gave a different set of parameters. While the 11 assigned Γ_5 levels led to an *rms* deviation of 62 cm^{-1}, the 11 Γ_1 levels were fitted with an *rms* deviation of 72 cm^{-1}. Finally the best fit for the 22 levels together was obtained with the starting values for the Γ_1 levels. From the calculated energy levels, 30 transitions could be assigned with good agreement between the calculated and measured energies. The B_q^k were first varied, then the F^k and ζ parameters. Finally all the parameters were varied simultaneously. For the fit with 30 levels an *rms* deviation of 77 cm^{-1} was obtained with 11 parameters varying. In this fit three levels could not be well fitted, the Γ_5 level at 19 529 cm^{-1} and the two ground state Stark levels $^3H_4$ at 473 and 623 cm^{-1} attributed to Γ_1 states. Moreover 4 strong π lines in the region of the $^3P_0$ (14 500-14 600 cm^{-1}) could not be attributed to calculated levels. The calculated energy levels and eigen vectors are given in table V and the final values of the parameters are given in table VI.

Compared with the spectroscopic parameters of U^{4+} in β-$ThBr_4$ [10] and β-$ThCl_4$ [22], the calculated parameters of U^{4+} in α-$ThBr_4$ are different, particularly B_0^2 which is smaller and the sign of B_0^4 and B_4^6 which becomes negative. If the *rms* deviation is not as good as in β-$ThBr_4$, the crystal field parameters are however determined with an uncertainty of about 10 % except B_0^6 and B_0^2. Moreover a decrease in the F^k parameters especially for F^4 is observed, which gives a ratio F^4/F^2 smaller compared to the values obtained for β-$ThBr_4$.

The Auzel parameter [28] N_v can be introduced to give a relative measurement of the crystal field

$$\frac{N_v}{\sqrt{4\pi}} = \left(\sum_{k,q} \frac{1}{2k+1} (B_q^k)^2 \right)^{1/2}.$$

Table V. — *Calculated and experimental energy levels of* α-$ThBr_4 : U^{4+}$.

Γ	E_{calc}	E_{obs}	ΔE (cm^{-1})	Eigen vectors	g_{calc}
4	0.0	0.0	0.0	$90\ ^3H_4 + 9\ ^1G_4$	
5	184.8	110.0	74.8	$87\ ^3H_4 + 11\ ^1G_4$	3.911
3	605.5	—		$86\ ^3H_4 + 10\ ^1G_4$	
5	831.3	830.0	1.3	$88\ ^3H_4 + 10\ ^1G_4$	− 0.379
1	843.2	—		$83\ ^3H_4 + 12\ ^1G_4$	
2	985.2	—		$89\ ^3H_4 + 9\ ^1G_4$	
1	1 008.6	—		$91\ ^3H_4 + 8\ ^1G_4$	
4	3 762.5	—		$78\ ^3F_2 + 11\ ^1D_2 + 9\ ^3H_5$	
3	3 966.5	—		$79\ ^3F_2 + 10\ ^1D_2$	
5	4 016.1	—		$83\ ^3F_2 + 12\ ^1D_2$	− 1.491
1	4 049.4	—		$79\ ^3F_2 + 15\ ^1D_2$	
5	5 780.7	—		$96\ ^3H_5 + 1\ ^3F_3$	4.38
4	5 797.0	5 765.0	32.0	$98\ ^3H_5$	
2	5 926.0	—		$96\ ^3H_5 + {}^3F_3$	
1	5 999.5	6 076.0	− 76.5	$96\ ^3H_5$	
1	6 316.6	6 362.0	− 45.4	$95\ ^3H_5 + 2\ ^3F_3$	
5	6 339.8	—		$97\ ^3H_5 + 1\ ^3F_3$	− 1.160
4	6 549.4	—		$87\ ^3H_5 + 8\ ^3F_2$	
5	6 575.4	6 487.0	88.4	$93\ ^3H_5 + 2\ ^3F_3$	− 8.975
4	8 195.7	8 170.0	25.7	$81\ ^3F_3 + 8\ ^3F_4 + 6\ ^1G_4$	− 8.975
5	8 293.0	—		$79\ ^3F_3 + 7\ ^3F_4 + 6\ ^1G_4$	4.096
3	8 323.4	—		$94\ ^3F_3 + {}^{33}H_6$	
2	8 542.1	—		$84\ ^3F_3 + 5\ ^1G_4 + 5\ ^3H_5$	
5	8 587.7	8 558.0	29.7	$71\ ^3F_3 + 9\ ^3F_4 + 8\ ^1G_4$	1.678
5	8 673.0	—		$32\ ^3F_4 + 30\ ^1G_4 + 26\ ^3F_3$	3.836
4	8 690.5	—		$43\ ^3F_4 + 31\ ^1G_4 + 14\ ^3F_3$	
1	8 975.9	8 972.0	3.9	$43\ ^3P_3 + 37\ ^1G_4 + 11\ ^3H_4$	
3	9 009.7	—		$49\ ^3F_4 + 37\ ^1G_4 + 9\ ^3H_4$	
2	9 131.2	—		$44\ ^3F_4 + 27\ ^1G_4 + 10\ ^3F_3$	
1	9 145.4	—		$53\ ^3F_4 + 19\ ^1G_4 + 8\ ^3H_6$	
5 (a)	9 147.2	9 240.0	− 92.8	$43\ ^3F_4 + 30\ ^1G_4 + 12\ ^3F_3$	− 1.434
4	10 540.1	10 504.0	36.1	$90\ ^3H_6 + 5\ ^1I_6$	
5	10 643.0	10 647.0	− 4.0	$90\ ^3H_6 + 4\ ^1I_6$	− 3.089
1	10 774.4	—		$85\ ^3H_6 + 5\ ^3F_4$	
2	10 865.7	—		$84\ ^3H_6 + 6\ ^1G_4$	
5 (a)	10 978.7	11 020.0	− 41.3	$91\ ^3H_6 + 5\ ^1I_6$	− 9.126
3	11 172.4	—		$88\ ^3H_6 + 4\ ^1I_6$	
1	11 336.5	—		$85\ ^3H_6 + 7\ ^1I_6$	
5	11 422.0	—		$86\ ^3H_6 + 9\ ^1I_6$	− 0.949
4	11 529.8	—		$86\ ^3H_6 + 7\ ^1I_6$	
3	11 734.1	—		$85\ ^3H_6 + 8\ ^1I_6$	
3	14 341.8	14 329.0	12.8	$47\ ^1D_2 + 31\ ^3P_2 + 15\ ^3F_2$	
1	14 350.7	14 389.0	− 38.3	$41\ ^1D_2 + 25\ ^3P_2 + 12\ ^3F_2 + 6\ ^3F_4$	
4	14 433.6	14 355.0	78.6	$45\ ^1D_2 + 37\ ^3P_2 + 9\ ^3F_2$	
5	14 442.9	14 427.0	15.9	$41\ ^1D_2 + 34\ ^3P_2 + 8\ ^3F_2$	− 0.976
1	14 457.1	14 460.0	− 2.9	$83\ ^3P_0 + 6\ ^1S_0$	
5	15 060.4	—		$44\ ^3G_4 + 37\ ^1G_4 + 7\ ^1D_2$	4.981
1	15 387.4	15 423.0	− 35.6	$44\ ^3F_4 + 37\ ^1G_4 + 8\ ^1D_2$	
4	15 442.3	15 456.0	− 13.7	$45\ ^1G_4 + 44\ ^3F_4$	
3	15 476.7	—		$46\ ^3F_4 + 45\ ^1G_4$	
5	15 558.8	15 509.0	49.8	$47\ ^1G_4 + 43\ ^3F_4$	− 1.899

(a) Lines of which the assignment has been deduced from the fit.

Table V *(continued)*.

Γ	E_{calc}	E_{obs}	ΔE (cm^{-1})	Eigen vectors	g_{calc}
1	15 709.4	15 692.0	17.4	49 $^1G_4$ + 41 $^3F_3$	
				1 3 1	
1	16 127.8	16 067.0	60.8	47 $^1G_4$ + 39 $^3F_4$ + 6 $^1I_6$	
2	17 026.7	17 017.0	9.7	94 $^3P_1$ + 3 $^3F_4$	
5	17 105.9	17 083.0	22.9	95 $^3P_1$ + 3 $^3F_4$	− 2.966
1	18 993.1	—		76 $^1I_6$ + 7 $^3H_6$	
5	19 075.5	—		90 $^1I_6$ + 8 $^3H_6$	− 1.227
3	19 208.2	—		89 $^1I_6$ + 9 $^3H_6$	
4	19 453.7	19 439.0	14.7	91 $^1I_6$ + 8 $^3H_6$	
3	19 454.1	—		91 $^1I_6$ + 18 $^3H_6$	
4	19 945.7	—		92 $^1I_6$ + 5 $^3H_6$	
5	20 036.3	20 034.0	2.3	84 $^1I_6$ + 8 $^3P_2$	− 3.184
2	20 357.9	—		93 $^1I_6$ + 5 $^3H_6$	
5	20 369.1	—		91 $^1I_6$ + 5 $^3H_4$	− 1.465
1	20 712.2	—		88 $^1I_6$ + 4 $^3H_6$ + 4 $^1G_4$	
3	21 220.7	—		63 $^3P_2$ + 33 $^1D_2$	
1	21 366.9	21 601.0	− 234.1	63 $^3P_2$ + 32 $^1D_2$	
4	21 766.7	—		56 $^3P_2$ + 38 $^1D_2$	
5	22 049.3	22 064.0	− 14.7	50 $^3P_2$ + 38 $^1D_2$ + 7 $^1I_6$	− 2.747
1	36 933.4	—		92 $^1S_0$ + 7 $^3P_0$	

Table VI. — *Spectroscopic parameters for* U^{4+} *in* α-$ThBr_4$ *in comparison with those of* β-$ThBr_4$.

Spectroscopic (1) parameters cm^{-1}	α-$ThBr_4$: U^{4+}	β-$ThBr_4$: U^{4+} (2)	β-$ThCl_4$: U^{4+} (22)
F^2	41 529 (158)	42 253 (127)	42 752 (162)
F^4	36 114 (486)	40 458 (489)	39 925 (502)
F^6	23 953 (415)	25 881 (383)	24 519 (479)
F^4/F^2	0.87	0.96	
F^6/F^2	0.57	0.61	
ξ	1 757 (7)	1 783 (7)	1 808 (8)
α	32 (1)	31 (1)	30.4 (2)
β	− 644 (144)	− 644 (75)	− 492 (84)
γ	(1 200)	(1 200)	(1 200)
B_0^2	− 382 (73)	− 1 096 (80)	− 1 054 (117)
B_0^4	− 3 262 (197)	1 316 (146)	1 146 (200)
B_4^4	− 1 734 (164)	− 2 230 (85)	− 2 767 (147)
B_0^6	− 851 (334)	− 3 170 (379)	− 2 135 (404)
B_4^6	− 1 828 (163)	686 (246)	− 312 (227)
n	30	26	25
rms	77	36	46
N_v'	1 565	1 543	1 560

(1) The M^k and P^k values were fixed : $M^0 = 0.99$, $M^2 = 0.55$, $M^4 = 0.38$, $P^2 = P^4 = P^6 = 500$, γ value was fixed.

(2) P. Delamoye, K. Rajnak, M. Genet, N. Edelstein, *Phys. Rev. B* **28** (1983) 4923.

Though the parameters are very different from the β-form, the crystal field strength has almost the same value for α and β-$ThBr_4$ (Tab. VI).

This set of parameters however is not completely satisfactory because it is disturbing that three intense transitions (the two $^3H_4$ Stark levels at 473 and 623 cm^{-1} well determined from several fluorescence lines and the Γ_5 at 19 529 cm^{-1}) fit so poorly. Moreover the π line at 21 601 cm^{-1} has a discrepancy with the calculated level of 234 cm^{-1} which is much more than the average discrepancy (39 cm^{-1}). In fact this level fits very well when all the Γ_1 levels are fitted. From the studies of Naik [29], Auzel *et al.* [30] and Schoenes [31], we can assume that the proximity of the 6d band to the 5f ones could provoke an interaction between both configurations, which is not taken into account in the Hamiltonian. It could shift the energy of the highest levels Γ_1 (19 529 cm^{-1}) and Γ_1 (21 601 cm^{-1}). Many fits were tried from various starting parameters and particularly the one obtained for β-$ThBr_4$, but they result in poor agreement with all the levels. Another reason for these discrepancies can be due to the fact that the site symmetry for Th^{4+} in this matrix is S_4 and that we made the approximation of D_{2d} symmetry.

The difference obtained in the crystal field calculation between both matrices α and β-$ThBr_4$ indicates that, although tetravalent uranium ion is surrounded by the same ligands, the most important difference in the two forms namely the relative orientation of the coordination polyhedron within the structure, the distances U-Br and the angles Br-U-Br (Tab. VII) play an important role in the crystal field parameters.

Table VII. — *Principal bond distances* (Å) *and angles in the polymorphic forms of* $ThBr_4$ *and* β-$ThCl_4$ (Ref. [1]) α, β-$ThBr_4$.

Compound	d_A	d_B	θ_a	θ_B	c	a	c/a
α-$ThBr_4$	3.020	2.909	37.9°	69.5°	13.601	6.737	2.019
β-$ThBr_4$	3.12	2.85	32.8°	77.3°	7.964	8.934	0.891
β-$ThCl_4$	2.903	2.718	33.1°	78.0°	7.465	8.486	0.880

In the β-form, the axes of the polyhedron lie in the (100) plane of the unit cell while in the α-structure, the polyhedron has been rotated by about 45°, the c axis and the polyhedron axis lie somewhat outside the (110) planes. This rotation allows for a more efficient packing of the Br^- atoms in the α-form. Moreover, the metal ligand distances are approximately all the same for α-$ThBr_4$ while there exist two different Th-Br bond distances for β-$ThBr_4$. For α-$ThBr_4$ all the bond distances Th-Br can be seen as intermediate between the longest and the shortest ones in β-$ThBr_4$.

6. Conclusion.

The optical spectra of U^{4+} in α-$ThBr_4$ have been analysed with 30 transitions assigned in the D_{2d} approximation. Although both matrices α and β-$ThBr_4$ look similar, it appears that the spectroscopic properties of the uranium tetravalent ion are quite different from one matrix to the other. As a matter of fact, U^{4+} ions give very strong fluorescences in the visible and infrared region in the α form while only 2 weak fluorescence lines were observed in the β-form. On the other hand the crystal field parameters obtained in this study are very different from those calculated in the β-form. Since the same ligands surround the uranium ion, it seems that the change in the structure plays an important role for the crystal field even if the site symmetry in the α-form which is S_4 can be approximated by D_{2d}. It is interesting to show that a small change in the structure with the same ions produces an important change in the crystal field parameters and that this scheelite structure material induces so many intense fluorescence lines for U^{4+} as the others scheelites do for rare earth ions and tetravalent neptunium [17]. The fact that the highest energy levels of U^{4+} do not fit as well as the others could be due to 5f-6d configuration proximity.

Acknowledgments.

We wish to thank Dr. G. Goodman for helpful discussions and Dr. N. Edelstein for providing us with the matrix elements and least squares program.

References

[1] MASON, J. T., JHA, M. C., BAILEY, D. M. and CHIOTTI, P., *J. Less Common Met.* **35** (1974) 331.

[2] SCAIFE, D. E., *Inorg. Chem.* **5** (1966) 162.

[3] CHIOTTI, P., FULLER, J. E., DOCK, C. H. and JHA, M. C., *J. Less Common Met.* **31** (1973) 365.

[4] D'EYE, R. W. M., *J. Chem. Soc.* (1950) 2764.

[5] HUBERT, S., DELAMOYE, P., LEFRANT, S., LEPOSTOLLEC, M. and HUSSONNOIS, M., *J. Solid State Chem.* **36** (1981) 36.

[6] BERNARD, L., CURRAT, R., DELAMOYE, P., ZEYEN, C. M. E., HUBERT, S. and DE KOUCHKOVSKY, R., *J. Phys. C* **16** (1983) 433.

[7] MASON, J. T., JHA, M. C. and CHIOTTI, P., *J. Less Common Met.* **34** (1973) 143.
[8] HUSSONNOIS, M., KRUPA, J. C., GENET, M., BRILLARD, L. and CARLIER, R., *J. Cryst. Growth* **51** (1981) 11.
[9] DE KOUCHKOVSKY, R., LE CLOAREC, M. F. and DELAMOYE, P., *Mater. Res. Bull.* **16** (1981) 1421.
[10] DELAMOYE, P., RAJNAK, K., GENET, M. and EDELSTEIN, N., *Phys. Rev. B* **28** (1983) 4923.
[11] KRUPA, J. C., HUBERT, S., FOYENTIN, M., GAMP, E. and EDELSTEIN, N., *J. Chem. Phys.* **78** (1983) 2175.
[12] CONWAY, J. G., KRUPA, J. C., DELAMOYE, P. and GENET, M., *J. Chem. Phys.* **74** (1981) 849.
[13] GOURDJI, M., PENEAU, A., GENET, M. and GUIBE, L., *J. Mol. struct.* **111** (1983) 27.
[14] HUBERT, S. and SIMONI, E., Private communication.
[15] VISHWAMITTAR and PURI, S. P., *J. Chem. Phys.* **61** (1974) 3720.
[16] ESTEROWITZ, L., BARTOLI, F. J., ALLEN, R. E., WORTMAN, D. E., MORRISON, C. A. and LEAVITT, R. P., *Phys. Rev. B* **19** (1979) 6442.
[17] SHARMA, K. K. and ARTMAN, J. O., *J. Chem. Phys.* **50** (1969) 1241.
[18] PHILLIPS, W. and FELDMAN, J. M., *J. Chem. Phys.* **42** (1965) 2933.
[19] GENET, M., HUSSONNOIS, M., KRUPA, J. C. and GUILLAUMONT, R., *J. Lumin.* **12** (1973) 953.
[20] SIMONI, E., HUBERT, S. and GENET, M., to be published.
[21] GENET, M., DELAMOYE, P., EDELSTEIN, N. and CONWAY, J., *J. Chem. Phys.* **67** (1977) 1620.
[22] KHAN MALEK, C., KRUPA, J. C., DELAMOYE, P. and GENET, M., *J. Phys. France* **47** (1986) 1763.
[23] FLINT, C. D. and TANNER, P. A., *Mol. Phys.* **53** (1984) 429.
[24] DA GAMA, A. A. S., DE SA, G. F., PORCHER, P. and CARO, P., *J. Chem. Phys.* **75** (1981) 2583.
[25] JENSSEN, H. P., LINZ, A., LEAVITT, R. P., MORRISON, C. A. and WORTMAN, D. E., *Phys. Rev. B* **11** (1975) 92.
[26] WYBOURNE, B. G., Spectroscopic Properties of the Rare Earth (Wiley & Sons, New York) 1965.
[27] KHAN MALEK, C. and KRUPA, J. C., *J. Chem. Phys.* **84** (1986) 6584.
[28] AUZEL, F., *Mater. Res. Bull.* **14** (1979) 223.
[29] NAIK, R. C. and KRUPA, J. C., *J. Lum.* **31** (1984) 222.
[30] AUZEL, F., HUBERT, S. and DELAMOYE, P., *J. Lum.* **26** (1982) 251.
[31] SCHOENES, J., *Phys. Rep.* **63** (1980) 301.